Amide and Peptide Bond Formation: Interplay between Strained Ring Defects and Silanol Groups at Amorphous Silica Surfaces

(Article begins on next page)

18 October 2024

Amide and Peptide Bond Formation: Interplay between Strained Ring Defects and Silanol Groups at Amorphous Silica Surfaces

Albert Rimola [a],, Mariona Sodupe [a], Piero Ugliengo [b]*

[a]Departament de Química, Universitat Autònoma de Barcelona, 08193 Bellaterra, Spain

[b]Dipartimento di Chimica and NIS – Nanostructured Interfaces and Surfaces – Interdepartment Centre, Università degli Studi di Torino, Via P. Giuria 7, 10125 Torino, Italy

Corresponding Author:

*E-mail: albert.rimola@uab.cat

*Tel: 0034-93-581-2164

ABSTRACT

Formation of amide and peptide bonds on plain amorphous silica surfaces is studied by DFT-D3 methods on cluster silica surface models envisaging strained Si-O rings as sources of reactivity. The amide/peptide bond formation reaction resulted thermodynamically and kinetically favored compared to the gas-phase processes due to the co-presence of surface $(SiO)_2/(SiO)_3$ strained

1

ring defects, which result from high temperature treatment of silica, and spatially close SiOH silanol groups. Preliminary extended calculations involving ammonia and formic acid give the insights for the most promising reaction paths for the amide bond formation on the defective silica surfaces. These paths were also adopted to study the glycine di-peptide formation. The reactions proceed through two steps: i) silica ring opening by reaction with carboxylic acids forming a Si-O-C(=O)- surface mixed anhydride (SMA); and ii) reaction of SMA with amines to form the amide product. The key point of the overall reaction is the synergy between the strained Si-O rings and spatially close silanol groups: SMA formation forces carboxylic acids to be immobilized on the surface, whereas SiOH groups are effective mild Brønsted catalytic acidic sites through a silanol-assisted proton relay mechanism in the second step. These results provide some atomistic insights of recent experimental findings on the formation of amides catalyzed by bare silica surfaces.

Introduction

Silica-based materials are among the most abundant and important inorganic materials on the Earth's crust. Pure silica (SiO_2) consists of corner-sharing [SiO_4] tetrahedral units. The different ways in which they are interconnected give rise to the different silica polymorphs, including crystalline and amorphous/glassy silica materials. Bare silica surfaces expose both siloxane (Si-O-Si) and silanol (Si-OH) groups, whose ratio imparts different degrees of hydrophilic/hydrophobic character to the silica surface.[1]

Amorphous silica is widely used as a transition metal support in a large number of catalytic systems. The surface Si-OH groups are easily exchanged for Si-O-M groups (where M is a

catalytically active metal such as V, W, Mo or Cr) making metal-ion-functionalized silica an excellent and well-studied material in heterogeneous catalysis.[2-5] Notwithstanding, the intrinsic catalytic properties of bare unmodified silica surfaces are far less understood. Due to the natural abundance and low cost of silica, great efforts to find catalytic routes using plain silica are ongoing. A relevant example of this is the amide bond formation between carboxylic acids and amines,[6-7] one of the most prevalent reactions both in nature and in the pharmaceutical field.[8-10]

Formation of amides by condensation between amines and carboxylic acids (see Scheme 1a) envisages nucleophilic attack of the nitrogen atom of the amine NH_2 group to the carbon atom of the C=O group belonging to the carboxylic acid. This step is followed by elimination of one water molecule with formation of the NH-C=O amide bond. Current synthetic ways for amides adopt highly reactive activating reagents for the COOH group.[11-14] However, their applicability is limited by widespread use of expensive reagents, which, moreover, generate toxic/corrosive by-products and large quantities of waste. Formation of an amide bond between two amino acids giving a peptide (*i.e.*, peptide bond formation) is still nowadays one of the critical and not well-understood steps in the sequence of organizational events leading to the emergence of the first biopolymers relevant for the origin of life. The reaction in highly diluted water solutions is thermodynamically disfavored,[15] since amino acid condensation is followed by water elimination (*e.g.*, the enthalpy for the condensation of alanine and glycine to form the dipeptide alanyl-glycine in H_2O is 4.13 kcal mol^{-1} at 37 ºC and pH=7[16]). Moreover, the kinetics of the reaction is very slow, with times in the order of several centuries.[15, 17] The calculated free energy barrier for the gas-phase condensation of two glycines is of about 50 kcal mol^{-1}.[18-19] Along this line, J. D. Bernal,[20] and more recently L. Orgel[21] advocated the special role of minerals as promoters for the biopolymers formation as they contain proper adsorption sites that may: i) immobilize and

concentrate monomers and protect biopolymers from hydration; ii) induce a lowering of the activation barrier because of the presence of catalytic active sites.

Several experimental works have validated the amide and peptide bond formation on oxide minerals, such as polymerization of amino acids in the presence of clays,[22] and thermally-induced transformation of amino acids into peptides on silica surfaces.[23-24] Recently, Comerford et al.,[25] found that silica Kieselgel K60, upon thermal pretreatment at 700 ºC, efficiently catalyzes the amide bond formation between carboxylic acid- and amine-containing molecules at 120 ºC, and the catalytic power is restored by heating the sample again at 700 ºC. Adopting a different experiment setup, Martra et al.,[26] evidenced by in-situ spectroscopic techniques that successive addition of gas-phase glycine monomers onto silica surfaces (and also TiO_2 surfaces) resulted with the formation of oligopeptides up to 16 units. The fine details of a possible mechanism are still unknown, the main difficulty being the knowledge of the exact distribution of silica surface functionalities. For instance, at variance with the Comerford's procedure, the silica adopted by Martra's groups was heated at only 140 °C for 1h under vacuum (vide supra), thus implying a different surface functionality distribution between the two cases.

In a recent theoretical work[27] we showed that strained ring motifs of $(SiO)_2$ and $(SiO)_3$ (so-called S2R and S3R, respectively, see Scheme 1b), present at silica surfaces due to silanol condensation reactions (*i.e.*, Si-OH + Si-OH $\rightarrow$ Si-O-Si + H_2O) occurring during thermal treatment at high temperature, can readily react with HCOOH leading to the opening of the rings by formation of one Si-OH group and a Si_{surf}-O-C(=O)-H surface mixed anhydride group (SMA). It was shown that the degree of the ring strain influences the energetics of the reactions: the larger the strain, the more favorable the ring opening process Along this line, Curtin and coworkers[28] showed with DFT methods that the structure and catalytic activity of silica-

supported metal catalysts largely depend on the size of the siloxane ring to functionalize. Moreover, in our work, electronic population analysis of the SMA moiety indicated that the electrophilic character of the carbon atom is increased compared to free HCOOH, enhancing the nucleophilicity which could help the amide bond formation. In the present work, we aim to assess. In this work, we aim to assess this hypothesis be means of quantum chemical calculations adopting the reaction shown in Scheme 1c. Moreover, we refine the previous models based on S2R and S3R by studying the role of a nearby silanol group on the amide/peptide bond formation, from both thermodynamic and kinetic aspects. It is worth noting that while S2R rings are only present at the silica surface in very small amount (less than 0.1 ring per nm^2) and after severe outgassing of silica (at T> 600 °C), the probability of occurrence of S3R rings in a bulk amorphous silica has been computed recently to be around 5%.[29] S2R rings are studied here as the highest strained case and accordingly they are not expected to play any practical role due to their negligible amount. Nonetheless, S3R rings, although not very abundant, may constitute a significant population to provide a decent number of reactive sites for the amide/peptide bond formations. This is particularly true for silica outgassed at high T, like in the Comerford's experiment with silica K60.[25] Here, we use quantum mechanical calculations based on DFT-D3 methods to preliminary study the formation of formamide from NH_3 and HCOOH and then, following the most favorable potential energy path, also for the condensation of two glycine molecules to form the glycylglycine dipeptide, the smallest prototype for peptide bond formation.

Methods

Calculations were run on cluster models mimicking the $(SiO)_2$ and $(SiO)_3$ strained ring motifs close to a single silanol group (hereafter referred to as S2R-SiOH and S3R-SiOH, respectively, and shown in Figure 1). The clusters were derived by secondary building units of microporous all silica zeolites to ensure enough rigidity in the models during geometry optimization. The S2R-SiOH cluster was modeled by joining three all-silica cages consisting of Si-O six-membered rings, in which the three cages are partly linked by the S2R defect (Figure 1a), whereas S3R-SiOH was modeled by joining laterally two cages of Si-O six-membered rings, linked through the S3R defect (Figure 1b). The level of strain of these rings is reflected by the calculated corresponding internal Si-O-Si angles (about 90 – 91 and 120 – 129 degrees, respectively, see Figure 1) indicating that S2R is highly strained whereas S3R shows moderate strain. The Si-O distances also reflect the larger strain of S2R than S3R, since they are larger in the former system (1.68 – 1.70 and 1.64 – 1.67, respectively, see Figure1).

All calculations were performed using the GAUSSIAN09 program.[30] To speed up the calculations, the structure of the reactants, transition states, and products were optimized using the ONIOM2[B3LYP/6-31+G(d,p):MNDO][31-34] method (see Figure 1). For consistency, reactant molecules were included in the high-level zone of the ONIOM2 calculations. The reaction energetics were refined by performing full B3LYP-D3/6-311++G(d,p) single point energy calculations on the optimized ONIOM2 stationary points, in which dispersion interactions are accounted for by including the Grimme's D3[35] correction term. Structures were characterized by the analytical calculation of the harmonic frequencies as minima (reactants and products) and saddle points (transition states). Free energies were computed including enthalpy and entropy contributions obtained at the ONIOM2 level to the B3LYP-D3/6-311++G(d,p)//ONIOM2 energies resulted from the standard rigid rotor/harmonic oscillator treatment.[36]

Results and Discussion

The uncatalyzed gas-phase amide bond formation can take place adopting either a concerted or a stepwise mechanism. In the concerted mechanism, the dehydration takes place because one H atom of the amine is transferred to the OH of the carboxylic acid, whereas in the stepwise one, the H is transferred to the O atom of the carboxyl CO group, giving rise to a di-alcohol intermediate. For the NH_3 + HCOOH reaction, the stepwise mechanism is energetically somewhat more disfavored (higher energy barriers) than the concerted one, and accordingly we based the reactions on the silica surfaces adopting a concerted-type mechanism.

In this part, we present first the results of the reactivity of the NH_3 and HCOOH on the S2R-SiOH cluster model, and then on the S3R-SiOH one. For this latter case, the reaction between two glycine molecules is also presented. Finally, a discussion of the match of our theoretical results with experiments of Comerford et al.[25] is presented.

Reactions on S2R-SiOH

Let us start with the S2R-SiOH case. The first step involves the reaction of the S2R site with HCOOH to form the SMA moiety. The computed free energy profile, shown in Figure 2a, is in agreement with previous works,[37-43] with favorable thermodynamic and kinetic aspects due to the high internal strain of S2R. A very low intrinsic free energy barrier (4.6 kcal mol^{-1} with respect to S2R_R) and a high exergonic character characterize the ring opening.

Formamide formation through reaction of the SMA intermediate (S2R_P structure) with NH_3, shown in Figure 2b, involves a nucleophilic attack of the N atom of NH_3 followed by the transfer of one H atom of NH_3 to the silica surface. However, such a proton transfer can be done through

different paths. One path implies a direct proton transfer to the O atom of the Si-OC moiety (AF1_TS1 structure). This H transfer forces the breaking of the Si-OC bond, thereby releasing formamide, and the formation of a new SiOH group. This first path has a highly strained transition structure due to the formation of a fourth-membered ring, and accordingly the computed intrinsic free energy barrier is significantly high (41.9 kcal mol^{-1} with respect to AF1_R). One of the ways to reduce the tension of highly strained transition structures, which in turn infers a lowering of the energy barriers, is by increasing the nuclearity of the ring characterizing the transition structures. This is well-known in water-assisted mechanisms.[44] In these cases, water molecules help proton transfers adopting a proton relay mechanism, in which they bridge the processes of accepting/donating protons to their neighboring molecules, and at the same time, they reduce the strain of the transition structure rings. Here, water is not present, and the surface SiOH groups play a similar proton relay mechanism. Thus, in an alternative path, the proton is transferred to the O atom of the vicinal SiOH group, which in turn releases its proton to the O atom of the Si-O-C moiety (see AF1_TS2 structure). Therefore, a silanol-assisted mechanism occurs. In this path, the transition structure envisages a sixth-membered ring and consequently the calculated free energy barrier is 30.2 kcal mol^{-1}, about 12 kcal mol^{-1} lower than the non-assisted reaction. Moreover, a third path adopting a similar silanol-assisted mechanism was found, in which the two surface SiOH groups, i.e., the vicinal and the isolated, participate in the proton transfer (AF1_TS3), thus adopting a doubly-silanol-assisted mechanism. This transition structure presents an eighth-membered ring giving a free energy barrier of only 21.0 kcal mol^{-1}, which is the lowest barrier among the three calculated paths. Therefore, the occurrence of silanol-assisted mechanisms exert dramatic effects on the computed free energy barriers similarly to the water assisted ones, *i.e.*, the less constrained the rings, the lower the

intrinsic free energy barriers. In summary, the calculated values are 41.9, 30.2 and 21.0 kcal mol⁻¹ for AF1_TS1, AF1_TS2 and AF1_TS3, respectively, with respect to AF1_R.

Remarkably, almost the same energy differences resulted when considering the purely potential energies (data available in ESI). It is worth pointing out that the non-assisted mechanism is somewhat activated towards the amide formation, since AF-TS1 exhibits a lower free energy barrier (∼10 kcal mol^{-1} lower) than the un-catalyzed gas-phase process (data available in ESI). This activation arises from the fact that the SMA functionality is engaged by H-bonds with the neighboring SiOH groups. Beside this, the actual catalysis is due to the participation of the SiOH groups in the reaction through a silanol-assisted process, while formation of SMA is mandatory to capture and firmly attach HCOOH. The three channels bring about the formation of two vicinal SiOH groups on the silica surface and formamide (see AF1_P). The free reaction energy is highly exergonic, with an intrinsic reaction free energy of -10 kcal mol^{-1}. This is in contrast to the computed values of about -3 kcal mol^{-1} for the uncatalyzed gas-phase reaction (see ESI), therefore suggesting that defective S2R rings at silica surfaces, in addition to reducing the energy barriers, favor the thermodynamics due to the H-bonding cooperative effects established between formamide and the three surface Si-OH groups.

We spend a word of caution related to the absolute validity of our calculations. It is well know that literature results about the opening of S2R by water action showed a sensitivity of the potential energy surface on both the adopted structural model (cluster vs periodic flat surfaces) and the computational method, as recently reviewed (Rimola et al Chem. Rev. 2013, 113, 4216-4313). A clear picture is still missing and we need more studies to deepen our understanding. Nonetheless, it is possible that the adoption of cluster models, as in the present study, when compared to S2R defect embedded in an extended periodic surface, would artificially increase

Reactivity on S3R-SiOH

S2R surface defects results from the condensation of two vicinal Si-OH sites; *i.e.*, HO-SiOSi-OH → $(SiO)_2$ + H_2O, during the thermal treatment of silica at T > 700 K. Silica samples activated at these high temperatures exhibit two infra-red bands at 888–891 and 908–910 cm^{-1}, which were assigned as the signature of the $(SiO)_2$ ring deformation modes.[45-49] However, the contact of the sample with 8–10 Torr of NH_3, H_2O or CH_3OH at room temperature causes these IR features to disappear immediately,[45, 49-51] which is attributed to the fast opening of the highly-strained S2R moiety. Because of that, S2R defects are only present in strict dry conditions and accordingly its concentration at silica surface is dramatically small (*vide supra*). This is at variance with $(SiO)_n$ rings with n > 2, such as S3R. These $(SiO)_n$ rings arise from condensation of non-vicinal interacting SiOH pairs upon moderate thermal treatment of the silica sample and are relatively stable, as the higher the ring nuclearity, the lower the strain and the higher their stability. Accordingly, and as already mentioned,[29] rings of this kind are more abundant at silica surfaces. Specific vibrational bands at 605–607 cm^{-1} for $(SiO)_3$ and at 131–133 cm^{-1} for $(SiO)_4$ have properly been characterized by Raman spectroscopy.[52-53] Thus, it is particularly interesting to check whether S3R rings behave differently from the S2R ones.

Figure 3a shows the $(SiO)_3$ ring opening by reaction of S3R-SiOH with HCOOH to form SMA (S3R_P). The process is thermodynamically and kinetically favorable, but the energetics are not as favorable as for the S2R-SiOH case; *i.e.*, the reaction free energy is less negative (although still highly favorable, -18.9 kcal mol^{-1}) and the free energy barrier is significantly higher (18.5

10

kcal mol^{-1}). Despite the energy barrier increase with respect to the S2R-SiOH case, the process is fast enough at normal conditions, since the classical Eyring equation for a first-order reaction gives a rate constant of 0.2 s^{-1} at 298 K, corresponding to a half-life time of about 4 s.

Figure 3b shows the reaction of the amide bond formation between S3R_P and NH$_3$. Here, we only calculated the non-assisted and the doubly-silanol-assisted mechanisms, as the two limiting cases. As in the S2R case, the non-assisted mechanism (AF2_TS1) presents a lower intrinsic energy barrier than the un-catalyzed gas-phase process. Furthermore, the calculated intrinsic energy barrier of the doubly-silanol-assisted mechanism (AF2_TS2) is 20.8 kcal mol^{-1} (close to its AF1_TS3 analogue, 21.0 kcal mol^{-1}), thus confirming the catalytic role of the silica surface due to the active role of the SiOH groups. The calculated rate constant and half-life time at 298 K associated with this process are about 3×10^{-3} s^{-1} and 211 s. Moreover, the reaction free energy is also favorable (-12.0 kcal mol^{-1}, see AF2_P) and, again, similar to AF1_P (-11 kcal mol^{-1}), confirming that the silica surface also favors the thermodynamics of the reaction due to H-bonding cooperative effects.

An interesting issue to explore here is whether similar results are obtained for the reaction between two glycine (Gly) molecules to form glycylglycine (GlyGly). This aspect is motivated by the fact that the acid/basic and nucleophilic/electrophilic characters of HCOOH and NH$_3$ are different from the -COOH and -NH$_2$ amino acid terminal groups. We only focused on the S3R ring, as it is the only case playing a possible role on the real material. Figure 4a shows the formation of the SMA surface group by reaction of one Gly with the S3R defect. The calculated intrinsic free energy barrier of the ring opening is 22.7 kcal mol^{-1} (see S3R_TS2), about 4 kcal mol^{-1} higher than the analogue process with HCOOH. The calculated rate constant and half-life time for this ring opening are about 1.4×10^{-4} s^{-1} and 4890 s ($\approx$82 min) at 298 K. This energy

barrier increase compared to the reaction with HCOOH is due to the fact that the Gly CO group is less electrophilic and its H proton less acidic than those of HCOOH. In the same line, the calculated reaction energy is less favorable than the HCOOH-analogue process but it is still negative (-6.6 kcal mol^{-1}, see SR3_P2). Figure 4b shows the reaction of the S3R_P2 structure with an incoming Gly molecule simulating the formation of the GlyGly peptide. Here we simulated this reaction only considering the doubly-silanol-assisted mechanism as it is kinetically the most favorable process compared to the non-assisted and the singly-silanol-assisted mechanisms. The calculated free energy barrier is 25 kcal mol^{-1} (see PF_TS), about 5 kcal mol^{-1} higher than the analogue amide bond formation process. This energy increase is in agreement with the respective SMA SiO-C distances (2.304 and 2.285 Å for PF_TS and AF_TS2, respectively), indicating that the latter structure presents a more reactant-like character. Despite this increase in energy, the doubly-silanol-assisted mechanism for the GlyGly formation dramatically decreases the energy barrier (a reduction of about 20 kcal mol^{-1}) compared to the un-catalyzed gas-phase process (see ESI for details). This reaction at 298 K is relatively slow as the calculated rate constant and half-life time are about 2.9×10^{-6} s^{-1} and 2.4×10^{5} s ($\approx$67 hours) but on a geochemical timescale it is actually very fast.

Match of the theoretical results with previous experimental findings

Our results may provide atomistic details for the experiments carried out by Comerford et al.[25] As mentioned above, these experiments identified a catalytic effect of the silica K60 towards formation of amides performed at 120 ºC when the silica sample was previously treated at 700 ºC. On one side, thermal pre-treatment at high T is essential to activate the silica surfaces through the formation of constrained S3R defects, which are reactive toward COOH-bearing

molecules to give SMA groups. The calculated free energy barriers associated with the S3R ring opening by reaction with HCOOH (S3R_TS1) and Gly (S3R_TS2) at 120 ºC (393 K) are 26.0 and 27.5 kcal mol^{-1}, respectively, giving rate constants and half-life times of 2.8×10^{-2} s^{-1} and 25 s, and 4.4×10^{-3} s^{-1} and 159 s (less than 3 min), respectively. The calculated free energy barriers for the formation of formamide (AF2_TS2) and GlyGly (PF_TS) operated at 120 ºC by the SiOH proximity are 22.8 and 31.8 kcal mol^{-1}, respectively, corresponding to the rate constants and half-life times of 1.7 s^{-1} and 0.4 s, and 1.8×10^{-5} s^{-1} and 3.9×10^{4} s (less than 11 h), respectively. Finally, experiments also show that the catalytic power of the K60 silica is restored when it is heated again at 700 ºC. We propose here that the need of this final heating is due to restoring the S3R rings at the silica surfaces in order to be operative for another set of reactions leading to the amide formation. To check this point, we have also calculated the re-formation of a S3R ring via condensation of two surface SiOH groups in S2_(SiOH)$_3$ (see Figure 5). This condensation at 298 K is both kinetically and thermodynamically unfavorable, with a free energy barrier as high as 29.3 kcal mol^{-1} and reaction energy of 4.6 kcal mol^{-1}. However, the process at 973 K has a free energy barrier of 32.2 kcal mol^{-1} (corresponding to an estimated rate constant of about 1.2×10^{6} s^{-1} ($\approx$25 min^{-1}) and a half-life time of 5.9×10^{-7} s) and a reaction free energy of -23.2 kcal mol^{-1}, which is entropically favored due to the H$_2$O molecule release. These results indicate that the ring closure is both thermodynamically and kinetically favorable at this temperature and accordingly the S3R can be reformed to react again with incoming carboxylic acids and amines.

Conclusions

Present results provide atomistic insights of the amide bond formation from carboxylic acids and amines on silica surfaces. We demonstrated that the occurrence of the reaction is in principle

possible due to a fruitful interplay between strained ring defects and silanol groups present at silica surfaces. The strained silica rings are reactive toward COOH-bearing molecules to give SMA groups. The amide bond formation completes by reaction of SMA with NH_2-bearing molecules. However, direct reaction with silica rings is not enough for its occurrence. The proximity of SiOH groups to the SMA moiety is essential for a catalytic effect based on a silanol-assisted mechanism that dramatically reduces the energy barrier compared to both gas-phase and other SiOH unassisted channels. This interplay is similar to that already identified by us[18] in the condensation of two glycine molecules on aluminosilicate surfaces presenting both Lewis and Brønsted acidic sites, in which the Lewis site binds the glycine to the surface and the Brønsted site performs the acidic catalysis to release water and favor the nucleophilic attack by the second glycine. In the present work, the actual catalytic effect is exerted exclusively by the SiOH groups, whereas previous SMA formation is mandatory to firmly attach the COOH-bearing molecules to the surface. It is worth mentioning, however, that, according to this mechanism, there will be as many reactions as strained ring defects contained on the silica surface and thus the overall reaction is stoichiometric, in which one silica ring is the reaction site of one chemical transformation. It is worth noting that the intrinsic reactivity of $(SiO)_3$ silica rings for peptide bond formation was already suggested in 1996 by Larry Hench[54] through small cluster model using the semiempirical AM1 method. Nonetheless, he did not suggest the key role of nearby silanol groups highlighted in the present work.

ASSOCIATED CONTENT

Supporting Information.

The following files are available free of charge.

Structures and energy profiles of the gas-phase uncatalyzed reactions (NH_3 + HCOOH →

NH_2CHO + H_2O and 2Gly → GlyGly + H_2O). Absolute potential energies and thermochemical

corrections of all the structures. Relative potential, including ZPE corrections and free energies

of the reactions (PDF).

AUTHOR INFORMATION

Notes

The authors declare no competing financial interests.

ACKNOWLEDGMENT

REFERENCES

1.   Rimola, A.; Costa, D.; Sodupe, M.; Lambert, J.-F.; Ugliengo, P., Silica Surface Features and Their Role in the Adsorption of Biomolecules: Computational Modeling and Experiments. *Chem. Rev.* **2013,** *113*, 4216-4313.
2.   Copéret, C.; Comas-Vives, A.; Conley, M. P.; Estes, D. P.; Fedorov, A.; Mougel, V.; Nagae, H.; Núñez-Zarur, F.; Zhizhko, P. A., Surface Organometallic and Coordination

Chemistry toward Single-Site Heterogeneous Catalysts: Strategies, Methods, Structures, and Activities. *Chemical Reviews* **2016,** *116*, 323-421.

3.   Stein, A.; Melde, B. J.; Schroden, R. C., Hybrid Inorganic–Organic Mesoporous Silicates—Nanoscopic Reactors Coming of Age. *Adv. Mater.* **2000,** *12*, 1403-1419.

4.   Copéret, C.; Chabanas, M.; Petroff Saint-Arroman, R.; Basset, J.-M., Homogeneous and Heterogeneous Catalysis: Bridging the Gap through Surface Organometallic Chemistry. *Angew. Chem. Int. Ed.* **2003,** *42*, 156-181.

5.   Thomas, J. M.; Raja, R.; Lewis, D. W., Single-Site Heterogeneous Catalysts. *Angew. Chem. Int. Ed.* **2005,** *44*, 6456-6482.

6.   Komura, K.; Nakano, Y.; Koketsu, M., Mesoporous silica MCM-41 as a highly active, recoverable and reusable catalyst for direct amidation of fatty acids and long-chain amines. *Green Chem.* **2011,** *13*, 828-831.

7.   Al-Zoubi, R. M.; Marion, O.; Hall, D. G., Direct and Waste-Free Amidations and Cycloadditions by Organocatalytic Activation of Carboxylic Acids at Room Temperature. *Angew. Chem. Int. Ed.* **2008,** *47*, 2876-2879.

8.   Albericio, F., Developments in peptide and amide synthesis. *Curr. Opin. Chem. Biol.* **2004,** *8*, 211-221.

9.   El-Faham, A.; Albericio, F., Peptide Coupling Reagents, More than a Letter Soup. *Chem. Rev.* **2011,** *111*, 6557-6602.

10.   Valeur, E.; Bradley, M., Amide bond formation: beyond the myth of coupling reagents. *Chem. Soc. Rev.* **2009,** *38*, 606-631.

11.   Carpino, L. A., 1-Hydroxy-7-azabenzotriazole. An efficient peptide coupling additive. *J. Am. Chem. Soc.* **1993,** *115*, 4397-4398.

12.   Cvetovich, R. J.; DiMichele, L., Formation of Acrylanilides, Acrylamides, and Amides Directly from Carboxylic Acids Using Thionyl Chloride in Dimethylacetamide in the Absence of Bases. *Org. Processes Res. Dev.* **2006,** *10*, 944-946.

13.   Paul, R.; Anderson, G. W., N,N'-Carbonyldiimidazole, a New Peptide Forming Reagent. *J. Am. Chem. Soc.* **1960,** *82*, 4596-4600.

14.   Pearson, A. J.; Rosuh, W. R., *Handbook of Reagents for Organic Synthesis: Activating Agents and Protecting Groups*. Wiley: New York, 1999.

15.   Lambert, J.-F., Adsorption and polymerization of amino acids on mineral surfaces: a review. *Orig. Life Evol. Biosph.* **2008,** *38*, 211-242.

16.   Brack, A., From Interstellar Amino Acids to Prebiotic Catalytic Peptides: A Review. *Chem. Biodiv.* **2007,** *4*, 665-679.

17.   Radzicka, A.; Wolfenden, R., Rates of Uncatalyzed Peptide Bond Hydrolysis in Neutral Solution and the Transition State Affinities of Proteases. *J. Am. Chem. Soc.* **1996,** *118*, 6105-6109.

18.   Rimola, A.; Sodupe, M.; Ugliengo, P., Aluminosilicate Surfaces as Promoters for Peptide Bond Formation: An Assessment of Bernal's Hypothesis by ab Initio Methods. *J. Am. Chem. Soc.* **2007,** *129*, 8333-8344.

19.   Redondo, P.; Barrientos, C.; Largo, A., Peptide Bond Formation through Gas-phase Reactions in the Interstellar Medium: Formamide and Acetamide as Prototypes. *Astrophys. J.* **2014,** *793*, 32.

20.   Bernal, J. D., The Physical Basis of Life. *Proc. Phys. Soc.* **1949,** *62*, 597-618.

21.   Orgel, L. E., Polymerization on the Rocks: Theoretical Introduction *Orig. Life Evol. Biosph.* **1998,** *28*, 227-234.

22.   Ferris, J. P.; Hill, A. R.; Liu, R.; Orgel, L. E., Synthesis of long prebiotic oligomers on mineral surfaces. *Nature* **1996,** *381*, 59-61.

23.   Lambert, J.-F.; Jaber, M.; Georgelin, T.; Stievano, L., A comparative study of the catalysis of peptide bond formation by oxide surfaces. *Phys. Chem. Chem. Phys.* **2013,** *15*, 13371-13380.

24.   Jaber, M.; Georgelin, T.; Bazzi, H.; Costa-Torro, F.; Lambert, J.-F.; Bolbach, G.; Clodic, G., Selectivities in Adsorption and Peptidic Condensation in the (Arginine and Glutamic Acid)/Montmorillonite Clay System. *J. Phys. Chem. C* **2014,** *118*, 25447-25455.

25.   Comerford, J. W.; Clark, J. H.; Macquarrie, D. J.; Breeden, S. W., Clean, reusable and low cost heterogeneous catalyst for amide synthesis. *Chem. Commun.* **2009**, 2562-2564.

26.   Martra, G.; Deiana, C.; Sakhno, Y.; Barberis, I.; Fabbiani, M.; Pazzi, M.; Vincenti, M., The Formation and Self-Assembly of Long Prebiotic Oligomers Produced by the Condensation of Unactivated Amino Acids on Oxide Surfaces. *Angew. Chem. Int. Ed.* **2014,** *53*, 4671-4674.

27.   Rimola, A.; Ugliengo, P.; Sodupe, M., Strained ring motif at silica surfaces: A quantum mechanical study of their reactivity towards protic molecules. *Comput. Theor. Chem.* **2015,** *1074*, 168-177.

28.   Das, U.; Zhang, G.; Hu, B.; Hock, A. S.; Redfern, P. C.; Miller, J. T.; Curtiss, L. A., Effect of Siloxane Ring Strain and Cation Charge Density on the Formation of Coordinately Unsaturated Metal Sites on Silica: Insights from Density Functional Theory (DFT) Studies. *ACS Catalysis* **2015,** *5*, 7177-7185.

29.   Malani, A.; Auerbach, S. M.; Monson, P. A., Monte Carlo Simulations of Silica Polymerization and Network Formation. *J. Phys. Chem. C* **2011,** *115*, 15988-16000.

30.   Frisch, M. J.; Trucks, G. W.; Schlegel, H. B.; Scuseria, G. E.; Robb, M. A.; Cheeseman, J. R.; Scalmani, G.; Barone, V.; Mennucci, B.; Petersson, G. A., et al. *Gaussian 09*, Gaussian Inc.: Wallingford CT, 2013.

31.   Becke, A. D., Density-functional thermochemistry. III. The role of exact exchange. *J. Chem. Phys.* **1993,** *98*, 5648-5652.

32.   Dewar, M. J. S.; Thiel, W., Ground states of molecules. 38. The MNDO method. Approximations and parameters. *J. Am. Chem. Soc.* **1977,** *99*, 4899-4907.

33.   Lee, C.; Yang, W.; Parr, R. G., Development of the Colle-Salvetti correlation-energy formula into a functional of the electron density. *Phys. Rev. B* **1988,** *37*, 785-789.

34.   Vreven, T.; Morokuma, K., On the application of the IMOMO (integrated molecular orbital + molecular orbital) method. *J. Comput. Chem.* **2000,** *21*, 1419-1432.

35.   Grimme, S.; Ehrlich, S.; Goerigk, L., Effect of the damping function in dispersion corrected density functional theory. *J. Comp. Chem.* **2011,** *32*, 1456-1465.

36.   McQuarrie, D., *Statistical Mechanics*. Harper and Row: New York, 1986.

37.   Rimola, A.; Ugliengo, P., The role of defective silica surfaces in exogenous delivery of prebiotic compounds: clues from first principles calculations. *Phys. Chem. Chem. Phys.* **2009,** *11*, 2497-2506.

38.   Rimola, A.; Ugliengo, P., A quantum mechanical study of the reactivity of (SiO)2-defective silica surfaces. *J. Chem. Phys.* **2008,** *128*, 204702.

39.   Walsh, T. R.; Wilson, M.; Sutton, A. P., Hydrolysis of the amorphous silica surface. II. Calculation of activation barriers and mechanisms. *J. Chem. Phys.* **2000,** *113*, 9191.

40.   Du, M.-H.; Kolchin, A.; Cheng, H.-P., Hydrolysis of a two-membered silica ring on the amorphous silica surface. *J. Chem. Phys.* **2004,** *120*, 1044.

41.   Masini, P.; Bernasconi, M., Ab initio simulations of hydroxylation and dehydroxylation reactions at surfaces: amorphous silica and brucite. *J. Phys.: Condens. Matter* **2002,** *14*, 4133-4144.

42.   Mischler, C.; Horbach, J.; Kob, W.; Binder, K., Water adsorption on amorphous silica surfaces: a Car–Parrinello simulation study. *J. Phys.: Condens. Matter* **2005,** *17*, 4005.

43.   Chen, Y.-W.; Cheng, H.-P., Interaction between water and defective silica surfaces. *J. Chem. Phys.* **2011,** *134*, 114703.

44.   Chalk, A. J.; Radom, L., Proton-Transport Catalysis: A Systematic Study of the Rearrangement of the Isoformyl Cation to the Formyl Cation. *J. Am. Chem. Soc.* **1997,** *119*, 7573-7578.

45.   Bunker, B. C.; Haaland, D. M.; Ward, K. J.; Michalske, T. A.; Smith, W. L.; Binkley, J. S.; Melius, C. F.; Balfe, C. A., Infrared spectra of edge-shared silicate tetrahedra. *Surf. Sci.* **1989,** *210*, 406-428.

46.   Chiang, C. M.; Zegarski, B. R.; Dubois, L. H., First observation of strained siloxane bonds on silicon oxide thin films. *J. Phys. Chem.* **1993,** *97*, 6948-6950.

47.   Michalske, T. A.; Bunker, B. C., Slow fracture model based on strained silicate structures. *J. Appl. Phys.* **1984,** *56*, 2686-2693.

48.   Morrow, B. A.; Cody, I. A., An Infrared Study of Some Reactions with Reactive Sites on Dehydroxylated Silica. *J. Phys. Chem.* **1975,** *79*, 761-762.

49.   Morrow, B. A.; Cody, I. A., Infrared studies of reactions on oxide surfaces. 5. Lewis acid sites on dehydroxylated silica. *J. Phys. Chem.* **1976,** *80*, 1995-8.

50.   Bunker, B. C.; Haaland, D. M.; Michalske, T. A.; Smith, W. L., Kinetics of dissociative chemisorption on strained edge-shared surface defects on dehydroxylated silica. *Surf. Sci.* **1989,** *222*, 95-118.

51.   Morrow, B. A.; Cody, I. A., Infrared studies of reactions on oxide surfaces. 6. Active sites on dehydroxylated silica for the chemisorption of ammonia and water. *J. Phys. Chem.* **1976,** *80*, 1998 - 2004.

52.   Riegel, B.; Hartmann, I.; Kiefer, W.; Groβ, J.; Fricke, J., Raman spectroscopy on silica aerogels. *J. Non-Cryst. Solids* **1997,** *211*, 294-298.

53.   Wallace, S.; West, J. K.; Hench, L. L., Interactions of water with trisiloxane rings. I. Experimental analysis. *J. Non-Cryst. Solids* **1993,** *152*, 101-108.

54.   Hench, L. L., Life and death: the ultimate phase transformation. *Thermochim. Acta* **1996,** *280–281*, 1-13.

Scheme 1. (a) Reaction of the amide bond formation between carboxylic acids (R_1-COOH) and amines (R_2-NH$_2$). (b) Picture of the S2R and S3R defects. (c) Reaction studied in this work: the amide bond formation on silica surface containing strained ring defects (here represented by S3R) in which the surface mixed anhydride (SMA) functionality is formed as intermediate species.
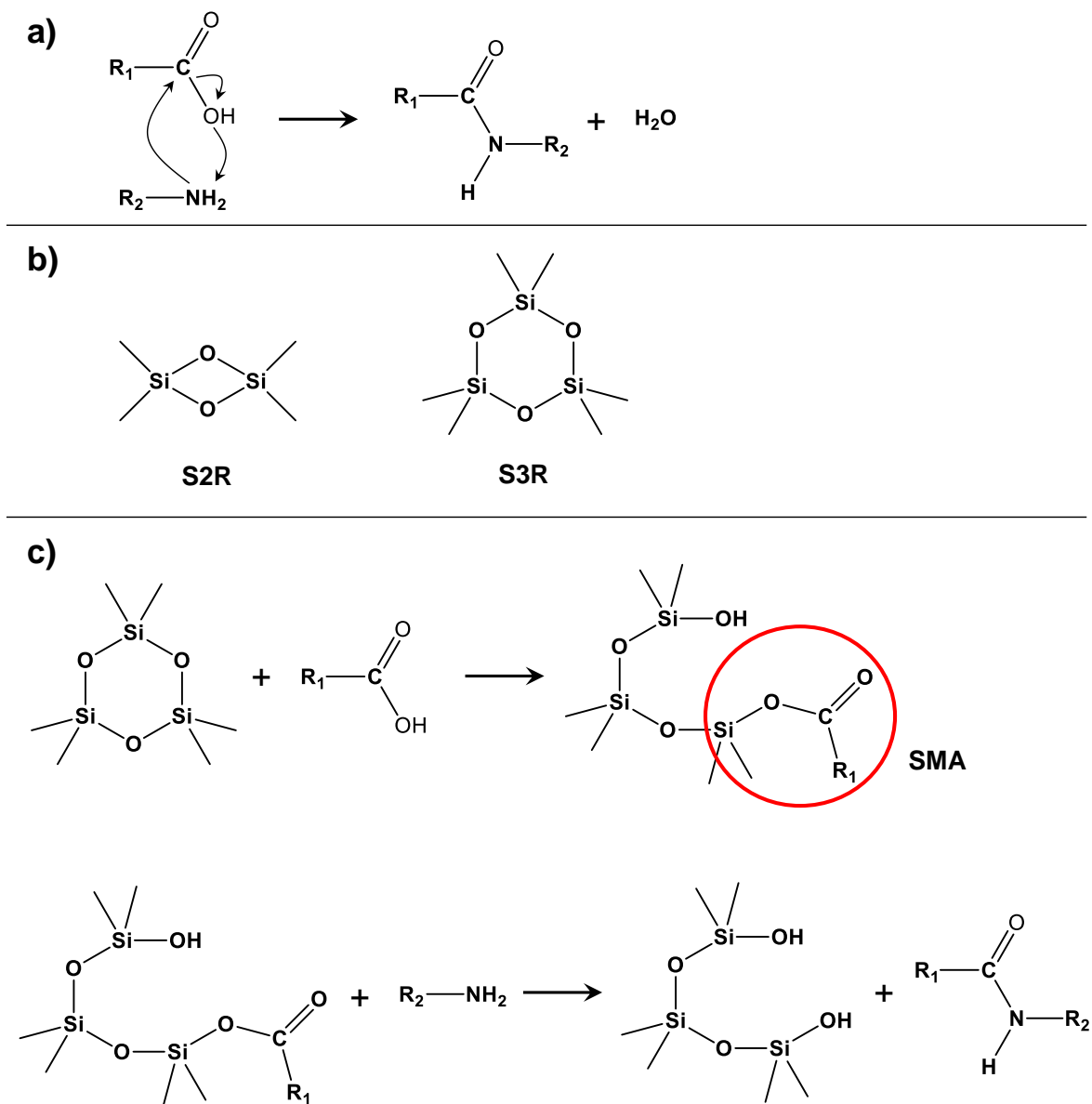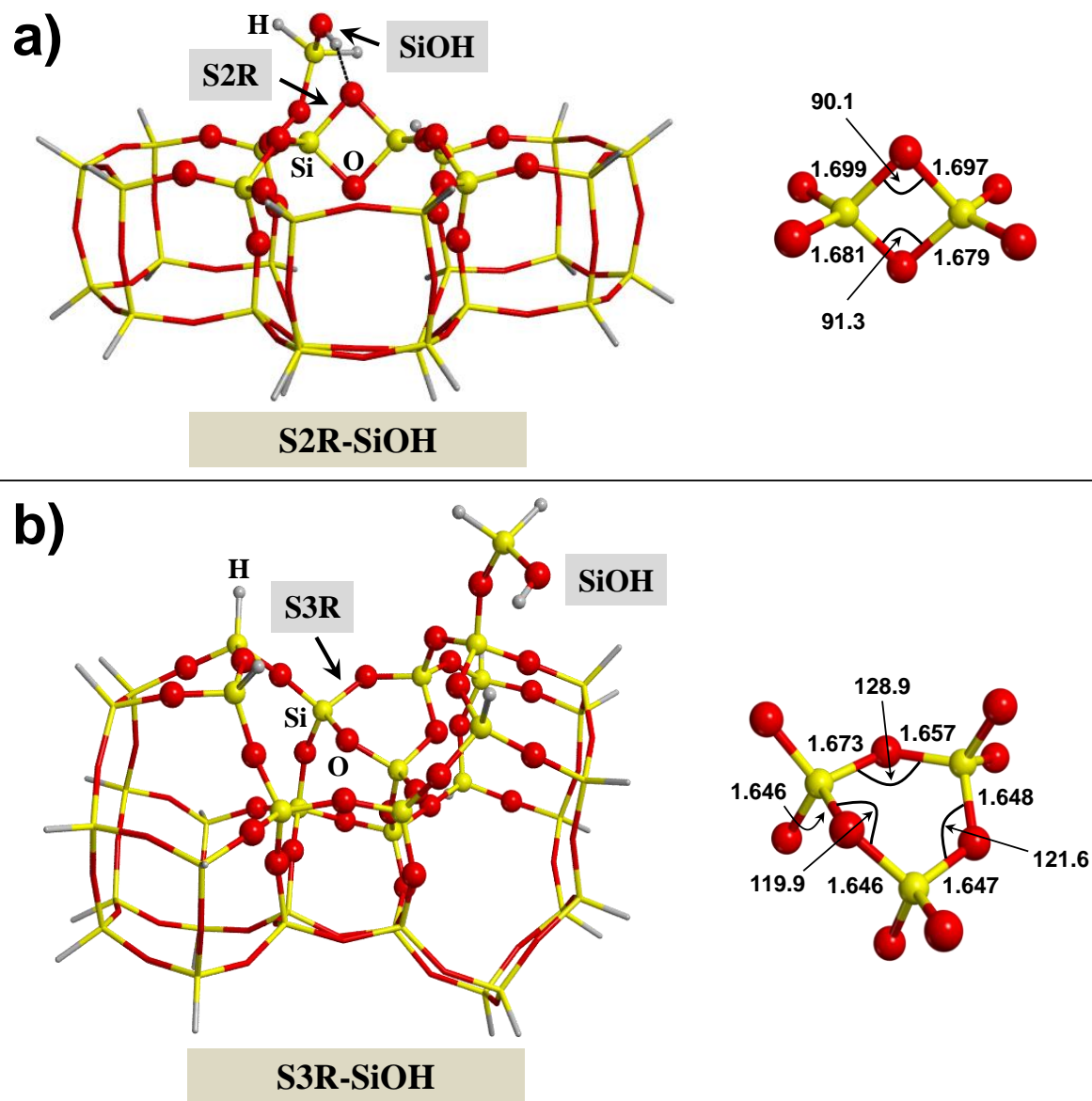
Figure 1. Clusters adopted to model the silica surfaces, which contain a S2R $(SiO)_2$ ring (a) or a S3R $(SiO)_3$ ring (b) and a nearby silanol (SiOH) group. Atoms shown as balls belong to the high-level zone in the ONIOM2 calculations and are treated at B3LYP/6-31+G(d,p). The real system is treated at the MNDO level. A zoom of the actual S2R (a) and S3R (b) defects is also provided, including the most relevant Si-O distances (in Å) and Si-O-Si angles (in degrees).
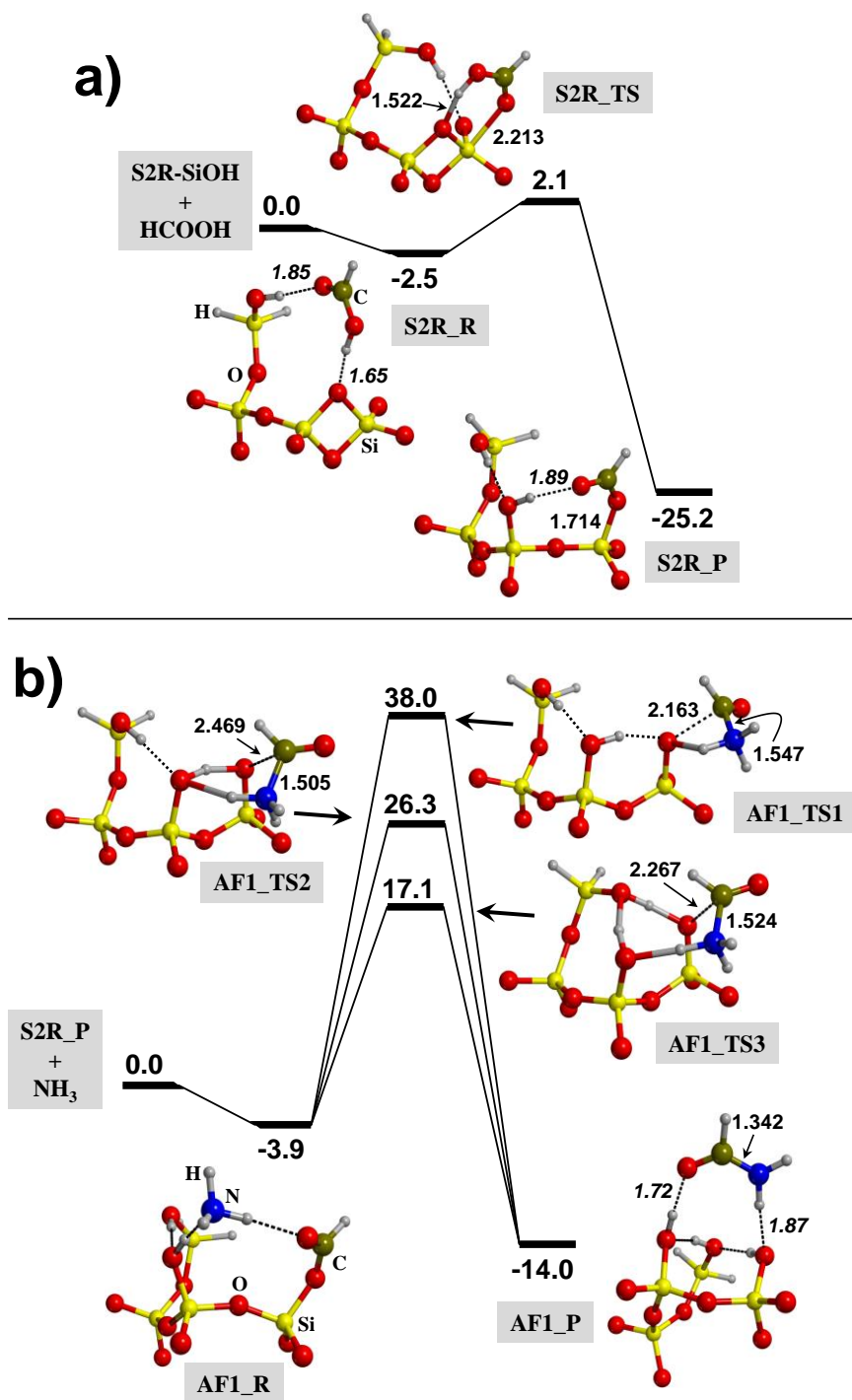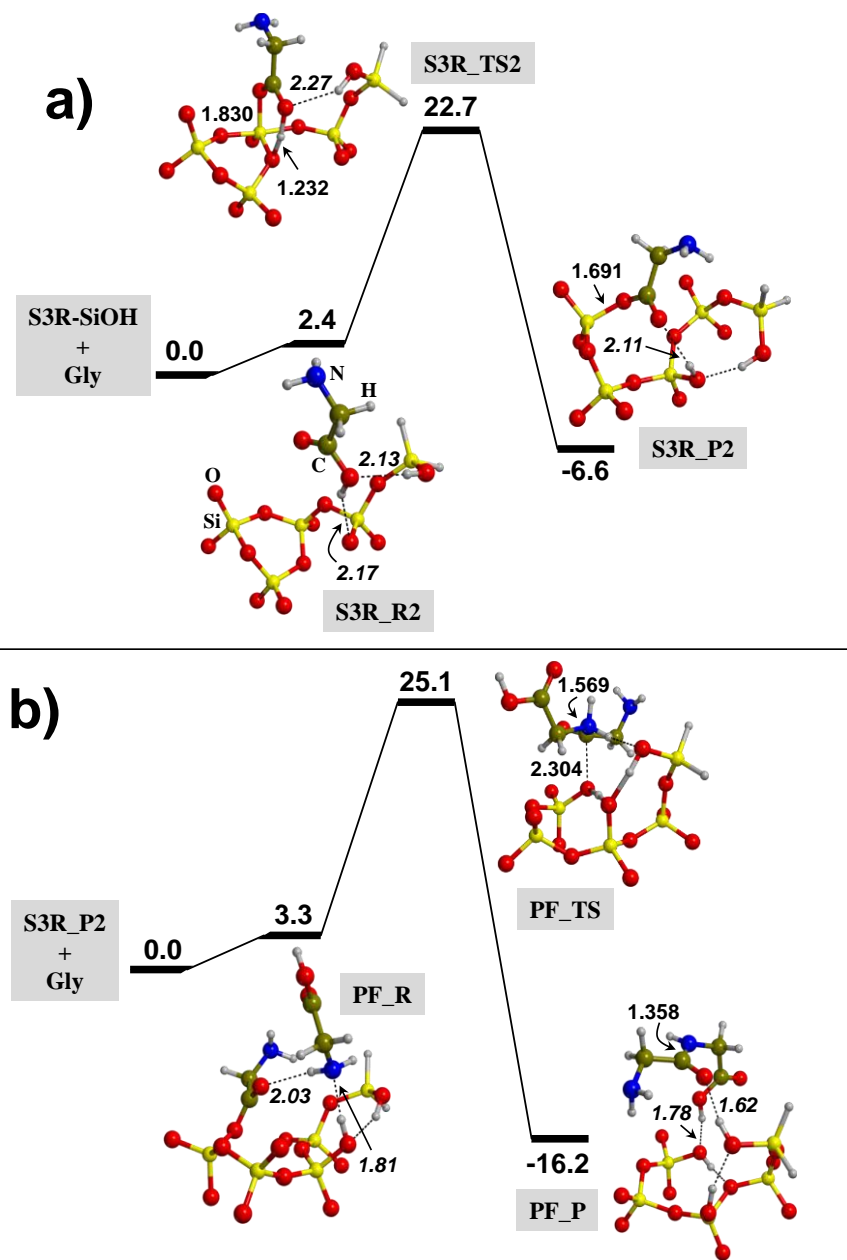
Figure 2. Relative free energy values at 298 K for the reaction of (a) the S2R-SiOH cluster model with HCOOH to form the Si$_{surf}$-O-C(=O)-H surface mixed anhydride group (values with respect to the S2R-SiOH + HCOOH asymptote), and (b) the amide bond formation between the surface mixed anhydride S2R_P and NH$_3$ (values with respect to the S2R_P + NH$_3$ asymptote). Energy units are in kcal mol^{-1} and bond distances are in Å.
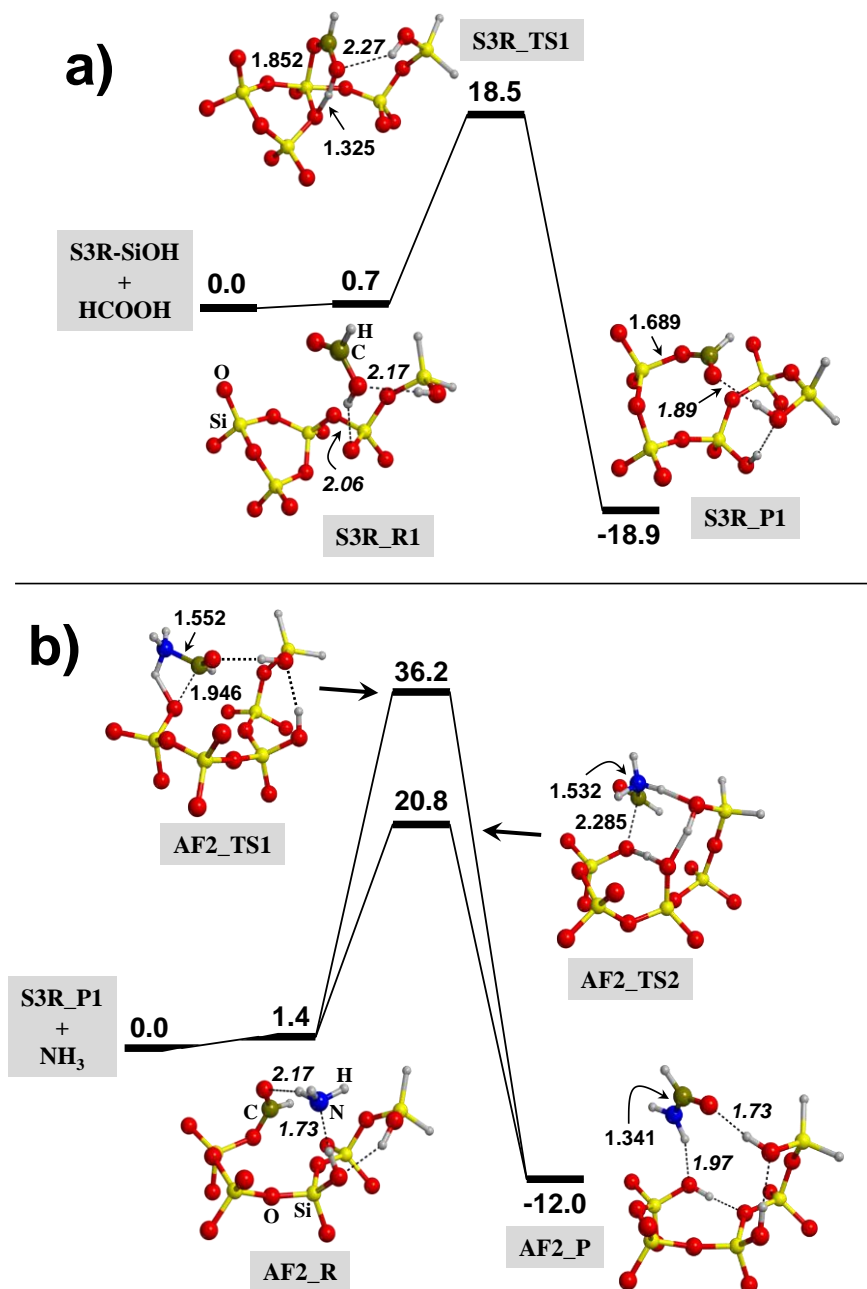
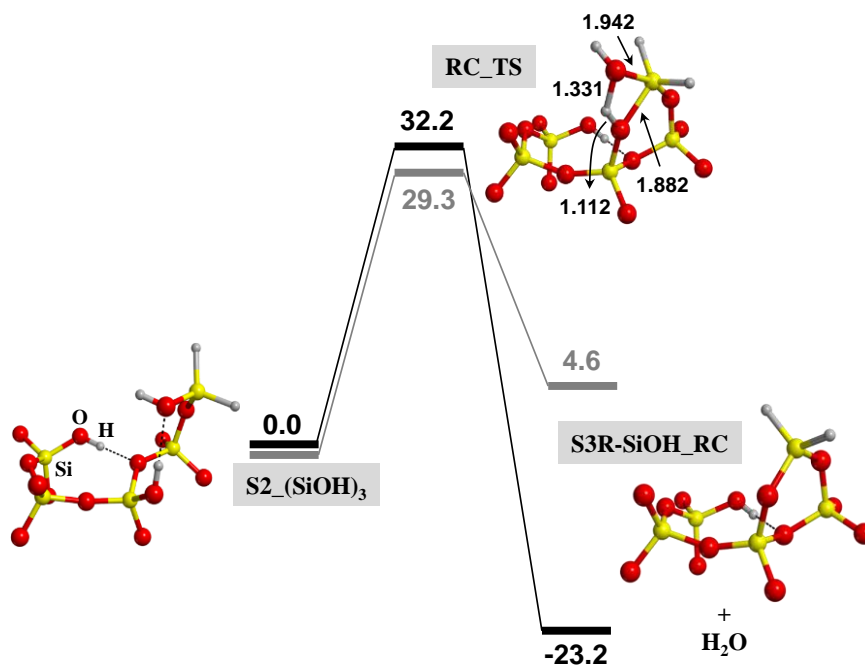**Figure 3.** Relative free energy values at 298 K for the reaction of (a) the S3R-SiOH cluster model with HCOOH to form the Si$_{surf}$-O-C(=O)-H surface mixed anhydride group (values with respect to the S3R-SiOH + HCOOH asymptote), and (b) the amide bond formation between the surface mixed anhydride S3R_P1 and NH$_3$ (values with respect to the S3R_P1 + NH$_3$ asymptote). Energy units are in kcal mol^{-1} and bond distances are in Å.

Figure 4. Relative free energy values at 298 K for the reaction of: (a) the S3R-SiOH cluster model with glycine (Gly) to form the Si_{surf}-O-C(=O)-CH_2-NH_2 surface mixed anhydride group (values with respect to the S3R-SiOH + Gly asymptote), and: (b) the peptide bond formation between the surface mixed anhydride S3R_P2 and a second Gly molecule (values with respect to the S3R_P2 + Gly asymptote). Energy units are in kcal mol^{-1} and bond distances are in Å.

Figure 5. Relative free energy values for the reaction of the ring closure from the $S2\_(SiOH)_3$ system. In grey calculated at 298 K, in black at 973 K. Energy units are in kcal mol^{-1} and bond distances are in Å.